University of Memphis
University of Memphis Digital Commons

Electronic Theses and Dissertations

7-1-2016

Cardiac Tissue Mapping Electrode Array to Determine Pro-Arrhythmic Tissue Substrates

Thomas Mark Shannon

Follow this and additional works at: https://digitalcommons.memphis.edu/etd

Recommended Citation
Shannon, Thomas Mark, "Cardiac Tissue Mapping Electrode Array to Determine Pro-Arrhythmic Tissue Substrates" (2016). *Electronic Theses and Dissertations*. 1432.
https://digitalcommons.memphis.edu/etd/1432

This Thesis is brought to you for free and open access by University of Memphis Digital Commons. It has been accepted for inclusion in Electronic Theses and Dissertations by an authorized administrator of University of Memphis Digital Commons. For more information, please contact khggerty@memphis.edu.

CARDIAC TISSUE MAPPING ELECTRODE ARRAY TO DETERMINE PRO-ARRHYTHMIC TISSUE SUBSTRATES

by

Thomas Shannon

A Thesis

Submitted in Partial Fulfillment of the

Requirements for the Degree of

Master of Science.

Major: Biomedical Engineering

The University of Memphis

August 2016

Copyright © Thomas Shannon

All rights reserved

Acknowledgements

This thesis is submitted as partial fulfillment of the requirements for a master's degree in biomedical engineering at the University of Memphis. It contains work done from September 2014 to March 2016 at the University of Memphis.

This thesis is written in its entirety by me, myself, and reviewed by my advisor Amy de Jongh Curry Ph.D.; however it does contain knowledge obtained from other scientists, and I have done my best to provide references to these sources.

I would like to thank Reginald Pruitt for his assistance, patience, and efforts to this research, as he was a vital part of the LabView programming. I would also like to express my gratitude for Dr. Curry for her guidance throughout the entire project. Without these two individuals this thesis would not have been possible.

I also want to thank my committee members Erno Lindner, Ph.D., Bashir Morshed, Ph.D., Judith Soberman, MD. for their insights toward this project. The unique blend of specialties and views enabled me to pursue this research in a complete manner.

Abstract

Myocardial infarction (MI), commonly known as a heart attack, is the irreparable necrosis of the cardiac tissue due to sustained ischemia. MI may lead to heart failure. Despite advances in treatments, the number of patients with heart failure is increasing. Engineered heart tissue, EHT, could offer an innovative approach to treating areas of infarcted cardiac tissue. Ideally, EHT should integrate and function with the native heart without causing a higher risk for complications. The purpose of this study is to design a system to identify potentially arrhythmogenic sites in EHT. Specifically, an electrode array complete with DAQ system and data analysis program was developed to record electrical propagation and interpret conduction velocity (CV) speeds to identify areas of slow conduction. This system has the ability to analyze the activation times, calculate CV vector fields, and identify areas within the mapping window that display slow CV speeds and are considered arrhythmic-prone.

Preface

This thesis is submitted in partial fulfillment of the requirements for a Master's Degree in Biomedical Engineering (BME). It contains work done from August 2014 to April 2016 at the University of Memphis.

This thesis has been entirely written by myself, Thomas Shannon, and reviewed by my advisor Dr. Amy de Jongh Curry. It contains knowledge discovered in previous experiments done by other scientists, and I have done my best to provide references to these sources.

I hope that the research and work done for this particular project promotes further questions and research for others as we continue to explore electrophysiology in the heart. I will introduce the reader to cardiovascular disease, in particular myocardial infarction and arrhythmia. I will also address the basic system design for cardiac mapping that maybe adjusted or enhanced for future research.

Table of Contents

List of Figures

I. Introduction

A. Myocardial Infarction

Myocardial infarction (MI), or more commonly known as a heart attack, is the irreparable necrosis of the cardiac tissue due to sustained ischemia. This lack of blood flow to an area of the heart can arise from many different sources such as coronary heart disease (CHD) and/or blood clots that block an artery to the heart [1]. MI is a life threatening condition that if not treated correctly could lead to heart failure. Approximately 1.5 million cases of MI occur annually in the US alone. The Global Burden of Disease study found that in 2010 an estimated 29.6% of deaths worldwide were caused by cardiovascular disease. In 2011, an MI was one of the top five most expensive inpatient hospitalizations in the US [2]. Currently, ischemic heart disease is the leading cause of death worldwide. According to the American Heart Association, about every 43 seconds, someone in the United States has a myocardial infarction [3].

An MI may lead to heart failure, arrhythmia, or cardiac arrest. Risk factors include, but are not limited to, diabetes, smoking, lack of exercise, obesity, high blood pressure, and high blood cholesterol. The most common symptoms of MI include chest discomfort, upper body pain that may spread beyond the chest to the arms, shoulders, back and neck, stomach pain that may mimic heartburn, shortness of breath, anxiety, dizziness, sweating, nausea and vomiting. Most heart attacks typically begin as discomfort rather than immediate pain and begin to increase in severity over the course of several minutes [6]. In 2005, 92% of respondents recognized chest pains as a symptom of heart attack and only 27% were aware of all of the major warning signs [7].

B. Post Myocardial Infarction Interventions

Identification and treatment after MI is critical for a successful recovery of the patient. Immediate intervention for this circumstance may include aspirin, diuretic, beta-blockers, other antiarrhythmic drugs, as well as the use of and electrical defibrillator for cases of severe arrhythmic episodes [1]. Depending on the extent of tissue damage, surgical procedures, such as RF ablation, or the use of an implantable device, such as a defibrillator or pacemaker, may be used [8].

Certain medications, in particular anticoagulants, are able to prevent blood clotting. This decreases both formation of new blood clots and continued growth of existing clots. These drugs have the ability to stop or decrease growth rate of existing blood clots, not break them down. The purpose of this particular treatment is to prevent the blood clots from moving into a location that would prevent oxygen to an area of the cardiac tissue. In order to decrease potential fluid accumulation, diuretic drugs are administered. Diuretics enable the body to reduce excess fluids and sodium through urination. This helps reduce blood pressure and reduce the heart's workload. This also prevents build up of fluids in the lungs and other parts of the body [9]. Beta-blockers, or beta-adrenergic blocking agents, are medications that help reduce blood pressure by inhibiting the effects of epinephrine. When beta-blockers are administered, the heart beats slower and with less force, thereby reducing blood pressure, chest pain, and the chance of mild arrhythmias. They are also able to help blood vessels relax which improves blood flow [10].

Depending upon the severity of the MI, angioplasty may be necessary. Angioplasty, also know as percutaneous coronary intervention, is used to physically widen a blood vessel where blood flow is restricted or blocked. This is accomplished by inserting a catheter with a uninflated balloon typically through the femoral or radial artery to gain access to the vascular

system. Once placed at the affected site, the balloon is expanded to enlarge the vessel and restore proper blood flow. Often times angioplasty is combined with the permanent placement of a stent, a small wired mesh tube, which helps keep the artery open [11].

There are more invasive procedures, including coronary bypass grafting, commonly referred to as bypass surgery. The aim is to divert the flow of blood around an artery that may be partially or completely blocked to improve blood flow to the cardiac tissue. For this procedure, a healthy blood vessel is taken from the patient's body, generally from the leg or arm. One end is connected to the coronary artery in the heart while the other is connected to the area where there is impaired blood flow so that oxygenated blood is able to bypass the blocked area [12,13].

In cases of severe MI, where normal pacing in the heart is altered leading to arrhythmia, the implantation of a pacemaker or implantable cardiac defibrillator, ICD, is necessary [14]. ICDs are small, battery powered devices that are implanted just under the skin. Leads from the subcutaneous device are inserted tranvenously and advanced into the cardiac tissue. ICDs operate by analyzing the electrical activity in the heart and deliver electrical shocks to restore normal rhythm if abnormal activity is detected [15].

C. Arrhythmia

A healthy heart's contraction cadence is essential for the efficient circulation of blood throughout the body. The heart has four chambers, the top two are called the atria, and the bottom two are called the ventricles. The atria, when relaxed, receive blood from the body and contract to move blood to the ventricles. After filling, the ventricles will then contract and push the blood to the body.

Contractions of the different chambers of the heart are controlled by the propagation of electrical signals called action potentials. The action potential wavefront in normal sinus rhythm propagates from the SA node, through the atria to the AV node, finally moving through the bundle branches and Purkinje fibers into the ventricles allowing for efficient contraction timing of the chambers in the heart and for effective blood flow. A cardiac arrhythmia is an irregularity with the rate or rhythm of the heartbeat. This abnormality can cause the heart to beat too slow, too fast, or with an irregular rhythm [16]. The electrical signals that would normally propagate through the cardiac tissue in a coordinated, timely manner now move chaotically through the tissue, causing irregular electrical activity in areas, and ill-timed contraction of the of the cardiac muscle. Spiral waves, rotors, or re-entrant circuits have become widely accepted as origins for many cardiac arrhythmias [17]-[20]. Connections between particular regions of the tissue may lead to the “current sink” or “current source” manifestation. Current sinks/sources occur when the excitability of a tissue region delivering the depolarization of the current, the source, is not equal to the excitability of the tissue region receiving the current, the sink [21] (Fig. 1). These electrical waves continually stimulate the tissue at a higher rate than normal sinus rate, inhibiting normal conduction in the tissue that can lead to arrhythmia [22]. Although slow conduction velocity (CV) may not be the only contributor to reentry in an infarcted area of the tissue, it does reduce the length of reentrant circuits and increases the chances for reentry [22].

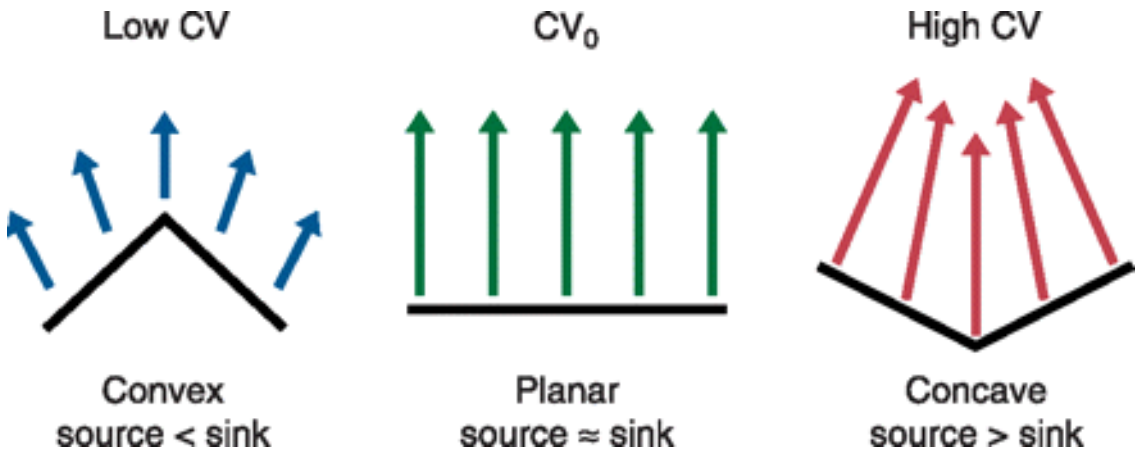

Fig. 1. This illustration from a fibrillation review by Schotten et al. [20] illustrates the direction of propagation for areas of cardiac tissue with varying conduction velocity (CV) speeds. It is important to understand that the electrical propagation of the heart depends on the balance between the "source" and "sink" of the depolarizing current. In a convex wavefront, leading cells activate more cells in front of it resulting in a small current source, a lower CV, and a greater potential for a reentrant circuit to occur. In concave wavefronts, many cells contribute to the activation of fewer downstream cells increasing CV [20].

D. Conduction Velocity

Action potential conduction is a product of complex interactions between cellular electrical activity, cardiac tissue structure, and electrical communication between cells. The CV of an action potential is vital in the ability for the heart to control the timing of contractions of the different chambers. The source-sink relationship, which represents the interactions between membrane elements (source) and tissue structure elements (sink), is important to consider when discussing CV and its significance in arrhythmia. Slowed CV in particular regions of the cardiac tissue is a marker of an underlying issue. There are multiple mechanisms associated with conduction slowing. These mechanisms include ischemia, scar tissue formation, cell shape, cell size, gap junction expression, and gap junction distribution [23]. These physical properties all have the ability to introduce an arrhythmia, making CV an important marker to determine arrhythmic prone sites in cardiac tissue.

E. Engineered Heart Tissue

Despite advances in both pharmacological and surgical treatments the number of patients with MI related deaths have not declined [24]. A marked reduction in quality of life and a high mortality rate due to heart failure in patients in not only the US but globally has stimulated the need for additional treatment strategies [25]. Engineered heart tissue, EHT, could offer an innovative approach to treating areas of infarcted cardiac tissue.

Scientists have developed patches of myocyte-seeded scaffolds that might be utilized to replace diseased areas of a living heart [26]. An EHT should integrate and function with the native heart both mechanically and electrically. The complete EHT will be contractile, mechanically durable/flexible, able to vascularize quickly upon implantation, and assimilate electrically into local cardiac tissue. Unfortunately, an EHT that encompasses all of these ideal characteristics has not yet been developed [27]. In essence, the cardiac tissue-engineering field is attempting to be able to replace diseased myocardium with prefabricated EHT. Multiple groups have been able to construct 3D EHT from neonatal rat heart cells in vitro [25]. The immediate issue that must be addressed is the functional properties of the EHT (mechanical function, vascular adaptation, electrical function, etc.) and if the EHT is a viable long term solution for diseased cardiac tissue. The result of the EHT's integration should result in improved cardiac function without inducing a higher risk for complications. The optimal EHT should have the ability to assimilate with the surrounding healthy tissue and maintain all essential cardiac tissue function [26].

The primary concerns are the ability of the EHT patches to improve function of the damaged cardiac tissue area and not serves as a catalyst for an arrhythmogenic site. If the EHT patch were conducting the action potentials slower than that of the surrounding healthy tissue,

then there would be an increased risk for developing an arrhythmia. Therefore, a valuable electrical characteristic to establish in the EHT is conduction velocity.

F. Current cardiac tissue characterization techniques

Cardiac mapping is a general term that includes different types of mapping techniques. These various techniques can include electrode arrays or sophisticated optical mapping techniques using voltage-sensitive dye and imaging systems with high temporal and spatial resolutions [28]. Electrophysiological studies of cardiac tissue often use isolated *ex vivo* characterization techniques that allow for controlled environments without the potential bodily interference that may compensate for certain situations in *in vitro* models; like the nervous system increasing heart rate via epinephrine [29].

Extracellular electrograms are considered the hallmark of invasive cardiac electrophysiology and provide essential information about the electrical activity in the underlying myocardium. An extracellular electrogram may be recorded from an electrode array in direct contact with cardiac tissue. The electrograms are created by the depolarization of the cardiomyocytes that generate transmembrane currents in the extracellular space. Under pathological conditions, however, electrograms may consist of unusual components that are attributed to abnormal CV [30]. In the case of *in vitro* analysis, a system to maintain physiologically relevant environment where pH and temperature are controlled is needed. Dulbecco's Modified Eagle Medium (DMEM, balanced salt solution) mixed with CO_2 has been previously used in order to provide a suitable environment as well as tissue viability [29, 31]. This bath system can also be used in-vivo and may be used to characterize pieces of cardiac tissue as well as EHT.

A successful *ex vivo* cardiac mapping experiment hinges upon two primary targets:

1. Tissue viability must be maintained in order to give relevant data. Perfusion technique, nutritional medium, O2-CO2 interaction to maintain pH balance, and temperature control can be used to ensure normal tissue function.
2. Comparative analysis of current and past electrical conduction in tissue sample results to determine effectiveness of environment control.

Previous work at University of Memphis has produced an inexpensive and simple tissue bath system to maintain a physiologically relevant environment for isolated *ex vivo* cardiac tissues [29], a data acquisition system to record extracellular electrograms, and data analysis software to determine activation time of the tissue [32]. Activation time data was then processed offline to give CV characteristics of the tissue [29].

G. Objectives

The overall objective of this study is to develop a cardiac mapping system to reliably determine activation time sequences in cardiac tissue samples. From these calculations, we determine CV for the tissue sample and translate that information into conduction characteristics and characterize areas of the cardiac tissue sample that display abnormal or arrhythmic prone traits.

Project objectives include:

1. Construct an inexpensive and simple electrode array that can be used to interact with cardiac tissue samples.
2. Develop a data acquisition and analysis system that can be used to determine activation times of the tissue, calculate CV, and identify and flag areas of the tissue that display abnormal conduction tendencies.
3. Perform experiments using porcine cardiac samples to evaluate the performance of our system on the response of the tissue to current stimuli.
4. Expand and update the previous methods in the lab of cardiac tissue characterization.

The method of cardiac tissue analysis via electrode mapping array along with an analysis program to determine regions of abnormal conduction in semi-automated will serve as a valuable tool to identify arrhythmic prone regions within the tissue sample. This method may have the ability to be expanded or refined to act as an EHT screening device.

II. Methods

The methods followed in this project were from a recognized standard from researchers and scientists in cardiac mapping [31]. These practices include determining stimulation/response threshold values, activation time calculations, as well as CV characteristics. Initial methods directly follow work previously performed in the lab by Villa [29].

A. Tissue bath development

A rectangular acrylic chamber used in previous studies was used as the tissue bath system chamber. Tissue clamps anchored to the bottom of the chamber hold the tissue samples in place during stimulation and recording. Physiological temperature was maintained by setting the chamber in a water bath continually heated via a ceramic hotplate. The chamber was filled with DMEM (Lonza BioWhittaker™ Dulbecco's Modified Eagle's Medium from Fisher Scientific) to a level that completely submerged the tissue by 1-2 mm [29,31]. The DMEM was continuously circulated at 120 ml/min using a Masterflex tubing pump. Temperature was controlled inside the chamber at 37±0.5 °C by using the hotplate with controller (IKA® C-MAG HP7 and IKATRON® ETS-D5, respectively); water level inside the metal pan was filled to surpass the level of the medium within the chamber. Water must be monitored and added throughout the trial as evaporation occurs during the experiment. The pH was maintained between 7.32±0.04 by bubbling in CO_2 using an automatic pH controller (BL931700, Harvard Apparatus).

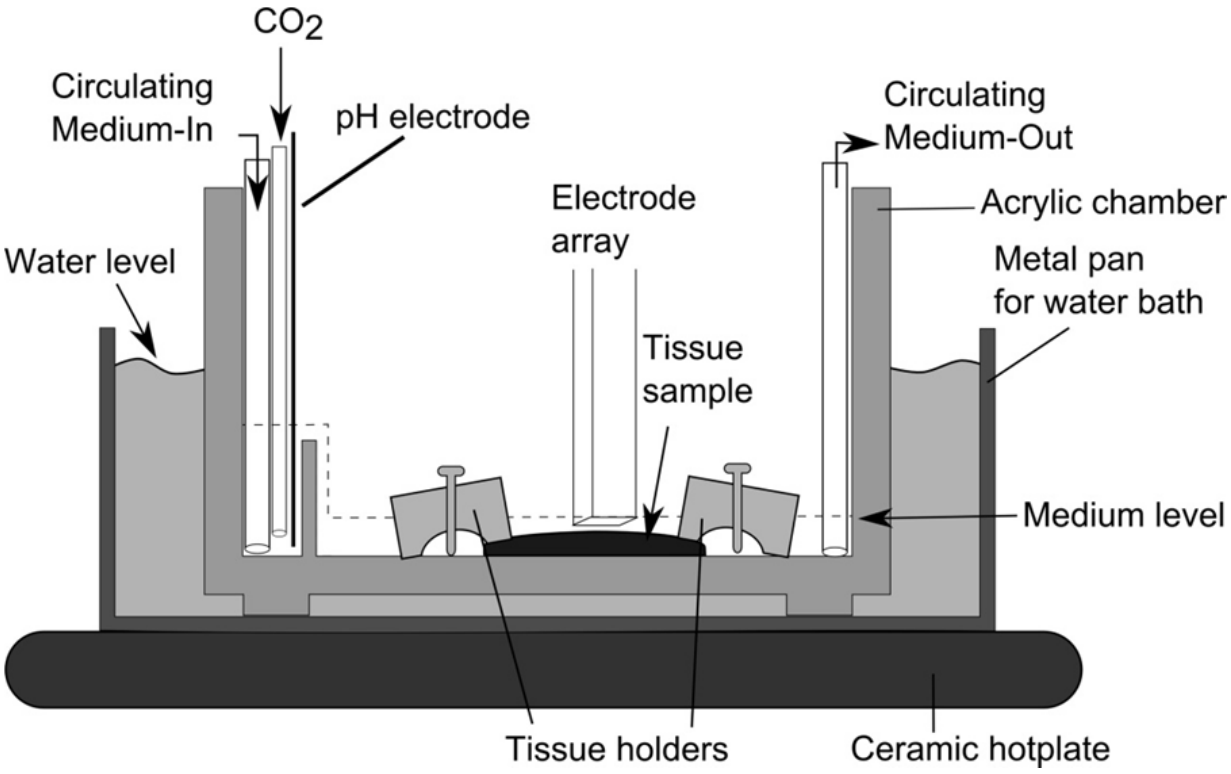

Fig. 2. Cross-sectional view of the constructed tissue bath system to maintain appropriate physiological conditions for cardiac tissue samples [29].

B. Tissue sample preparation

Our system's ability to maintain appropriate physiological conditions was tested using porcine cardiac tissue. Porcine samples were acquired from Dr. Randal Buddington, Professor, School of Health Studies, University of Memphis. Piglet age varied from 5 weeks to 13 weeks. Piglets were euthanized using a cardiac and respiratory knockout, SomnaSol Euthanasia solution.

The freshly removed heart was immediately placed on ice and transported, in under ten minutes, to the lab for analysis. The heart was rinsed in warmed saline to help prevent potential blood clot formation that may interfere with electrical stimuli and data recording. Dissection involved removing both atria as well as the right ventricle. The left ventricle was cut through the interventricular wall to allow the tissue to lay flat with the epicardium of the left ventricle facing

upward and paced into the tissue bath system, completely submerged by the DMEM solution, secured by the tissue clamps, and allowed to settle for 5-7 minutes to stabilize. During this time, the tissue was continuously evaluated for viability; this assessment was based on color, texture, and firmness of the tissue. Experiment was ended when the tissue became hard or if no electrical response was observed following stimulation.

C. Electrical characterization of the cardiac tissue

Mapping system: The mapping system we developed consists of an array of 11x11 Ag/AgCl coated copper electrodes (Fig. 3 A), and a reference electrode (Fig. 3 B) connected to a data acquisition system with LabVIEW interface. Each tissue sample was stimulated, via current stimulation program developed in LabVIEW and driven through a current Output Module designed for CompacDAQ (NI 9265; 4-Channel, 0 mA to 20 mA, 16-Bit Analog Output Module; National Instruments, Austin, TX.). The system contains 3 modules (NI 9205; 32-Channel, ±200 mV to ±10 V, 16-Bit Analog Input Module; National Instruments, Austin, TX.) that use 27 channels for amplification and filtration each which produce 81 total electrical channels for data acquisition. Electrograms, in the form of analog signals, recorded from each of the electrodes within the 9x9-recording matrix are transferred individually through a Compact DAQ (NI-cDAQ 9174; 16-Bit Analog NI CompactDAQ; National Instruments, Austin, TX.) to a Dell Optiplex GX620 computer where data is collected and displayed as individual electrograms. These electrograms are then processed through a programmed LabVIEW interface where two-dimensional electrical characterization analysis is performed.

A. 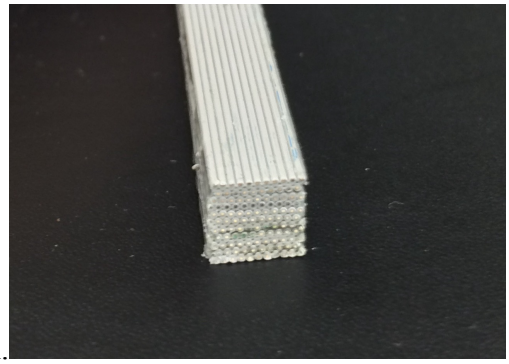 B. 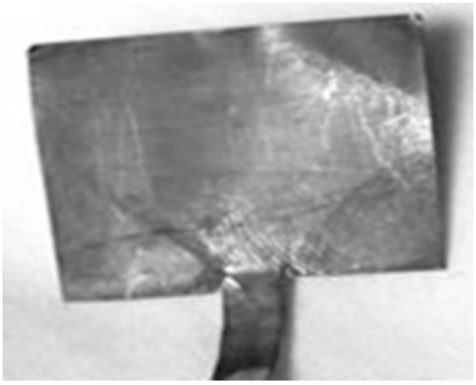

Fig. 3. (A) Electrode array: 9x9 recording electrode matrix, 0.254 mm electrode diameter, 0.61 mm separation between electrodes. **(B)** Reference electrode (28 mm x 34 mm) was constructed from silver foil and electroplated (Ag/AgCl) [29].

Stimulation and mapping protocol: The protocol for stimulation and mapping followed previous efforts in the lab by Villa [29]. The pacing threshold was found by delivering a square wave stimulus, 3 ms pulse width, at 1 Hz for 5 s, from a line of electrodes that borders one side of the electrode array. The initial amplitude for the stimulus started at 0.5 mA and was increased by 0.1 mA until tissue activation was achieved (Fig. 4 and Fig. 5). Once a pacing threshold was verified, the tissue samples were stimulated at 1.5 times the pacing threshold value and electrograms were recorded for episodes of 20 s. After successful tissue activation and recording, temperature and pH levels were recorded to continually maintain applicable physiological conditions.

Fig. 4 A-C were obtained from previous experiments [29] where tissue activation was achieved following current input. Due to the limited porcine samples tissue activation was not achieved in our experiments. Fig. 5 shows results from our efforts in the lab. Although tissue activation was not achieved the experiment, we successfully mapped electrical potential changes in all 81 of our mapping electrodes as well as successfully developed a current stimulation module that allowed us to manipulate the pulse width and amplitude of current input.

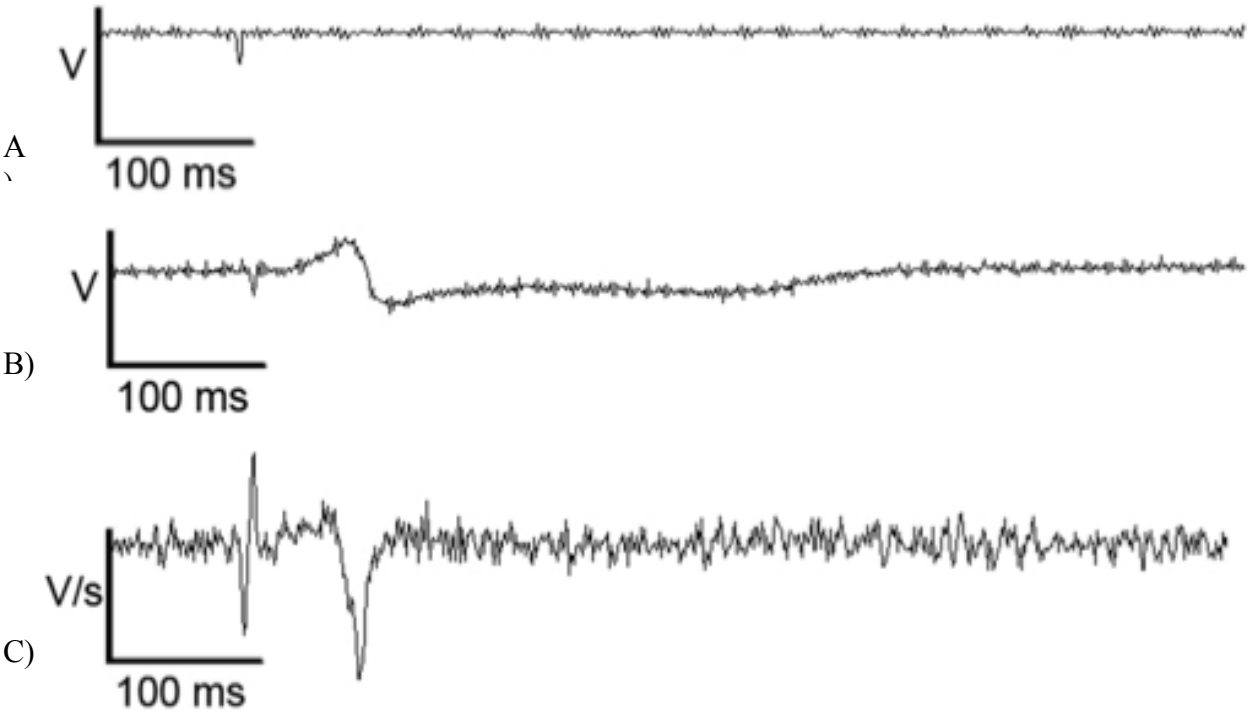

Fig. 4. (A) Electrogram recording from a porcine tissue sample at an electrode 8 mm (vertical distance) from the stimulation site from which a 0.7 mA stimulus was delivered. The large negative deflection is the stimulus artifact. (B) An active response was achieved after the stimulus artifact at the same electrode location as Fig. 3. The stimulus delivered was 0.9 mA, the activation threshold for this tissue sample. (C) The first derivative of the signal in (B) is shown. The first large negative/positive deflection corresponds to the stimulus artifact. The nadir of the second large negative deflection corresponds to the activation time for this response.

A
)

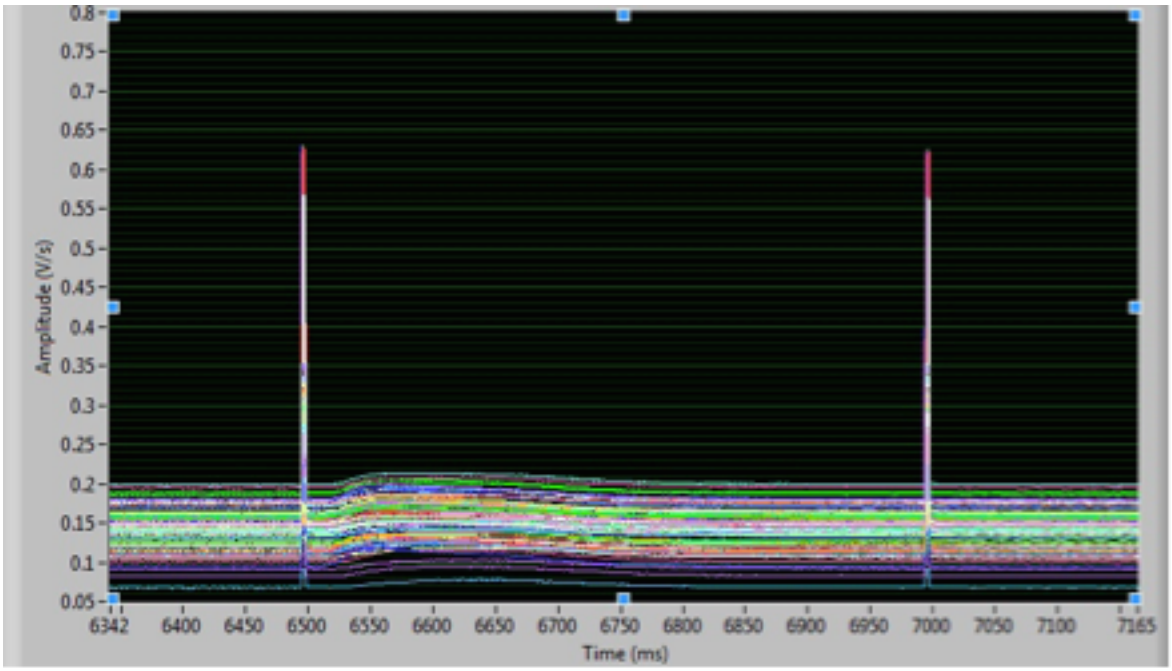

B)

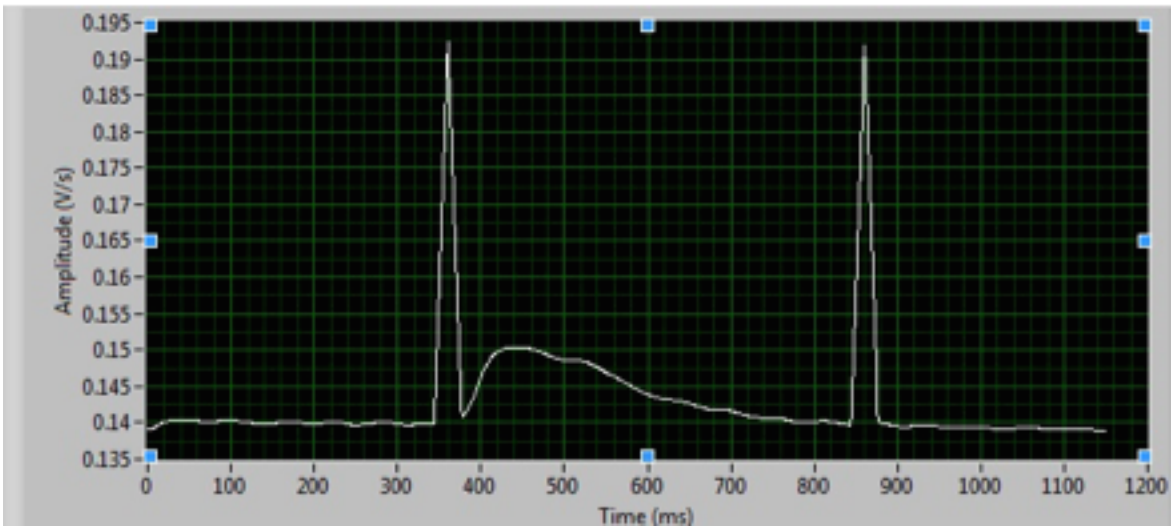

Fig. 5. (A) View of the user interface for all 81 mapping electrodes for the current LabVIEW program. The stimulus artifact is seen in all 81 of the mapping electrodes. There is no large deflection detected following the stimulation suggesting tissue activation was not achieved. Single (B) electrode view from (A). The LabVIEW program allows the user to individually monitor a single electrode. Again, the stimulus artifact is seen in the single electrode. There is a small deflection following the stimulus artifact. However, the amplitude as well as the duration of the deflection (>200 ms) suggests that it is not tissue activation.

D. Data Analysis

Electrograms for each of the individual electrodes were evaluated to determine if the underlying tissue was activated. The activation time for each electrode was found as the maximum negative value of the first derivative (dV/dt) from its respective electrogram during the pacing cycle (Fig. 4) [33]. An electrode was considered active if the maximum negative value was less than -0.5 V/s [34]. Pacing episodes data was analyzed for electrical wavefronts, and episodes that displayed an electrical wavefront across entire electrode array were selected for data analysis. These data sets were evaluated using a LabVIEW VI (Virtual Instrument) developed to analyze the electrode matrix data. The programed LabVIEW VI reviews the spatial distributions of activation times. If the activation time difference of a given electrode was greater than two standard deviations compared to the window of 3 to 6 surrounding electrodes, the value was considered an outlier and the value is eliminated. A MATLAB script was developed to import data from the LabVIEW VI that also displays relative activation times of each individual electrode as a contour plot, calculates conduction velocity speed and direction, and identify areas of the tissue that exhibit slow CV speeds that are considered arrhythmic prone.

Conduction velocity describes the local magnitude and direction of electrical propagation activity in the heart tissue and may fluctuate depending on tissue properties, fiber orientation, gap junction placement, and previous activity, all of which have the ability to change over time and significantly differ depending on location within the tissue [35]. The magnitude of conduction velocity was measured by determining the direction of propagation and calculating the distance a particular wave front travels over the difference in time of activation between two electrode points. After tissue activation times were determined for the individual electrodes, CV vectors representing the speed and direction of electrical propagation were calculated using a

MATLAB script. This MATLAB script uses previous methods provided by Bayly et al. [36]. The method uses spatial windows that are defined as six or more adjacent electrodes that have recorded activation times. The spatial windows are then projected as velocity vectors from the partial derivatives of fitted polynomials $T(x,y)$ to a data set of spatial activation points (x,y,t) using a least squares fitting procedure, where x and y are locational characteristics of the electrodes within the electrode matrix and t is the time the particular electrode was activated based on the criteria previously mentioned. An activation time contour plot and CV vector plot is displayed to allow for a quick analysis of the overall electrical propagation. The conduction velocity is then plotted into an intensity graph where speeds are represented as normal conduction speed (green), or slow conduction speed/arrhythmic prone site (red). Abnormal CV speed that is flagged using red is under 0.08 m/s. Areas that display CV speeds slower that 0.08 m/s are highly susceptible to reentrant circuits, a major cause of arrhythmia [40]. This allows for real time analysis and determines if/where an arrhythmic prone site is located within the electrode array portion of the cardiac tissue. The mean conduction speed for each pacing episode was calculated as an average of the magnitude of each velocity vector within the episode.

III. Results

This research investigates the capability of cardiac mapping system in two manners. First, the electrode array must be validated; the electrode array must drive a desired current through a line of electrodes as well as determine electric potential changes in individual electrodes to map electrical propagation on the surface of the tissue substrate. Second is the ability to determine activation times in each of the 81 mapping electrodes, calculate conduction velocities, and identify areas within the 9x9 mapping region that present arrhythmic prone CV speeds. Preliminary testing in saline solution procedure and results are shown in Appendix D.

A. Activation Thresholds

Activation thresholds are defined as the minimum stimulus amplitude required achieving a response from the tissue sample. The VI built in LabVIEW allows the user to manipulate both the amplitude, pulse width, duration of stimulus, and pulse interval of the current to create the desired current waveform. Amplitude for current in all five porcine experiments began with a current of 0.65 mA and a pulse width of 3 ms and was increased by 0.1 mA until 1.4 mA amplitude was reached. Activation thresholds for previous experiments performed by Villa [29] were found at 0.88±0.09 mA; however, due to the limited number of porcine samples available activation thresholds were not achieved.

B. Activation Time Identification and Conduction Velocity Analysis

Activation times for individual electrodes are necessary in determining both electrical wavefronts and conduction velocity. Previously, relative activation times were determined through extensive post processing by the user. Now, the LabVIEW VI that has been developed is

able to determine relative activation times of individual electrodes immediately following a pacing episode. This is achieved by a windowing mechanism that allows the investigator to select epochs of raw data to be analyzed and processed. Once a particular set of data is found and processed it is converted into a set of data for each electrode (X electrode position, Y Electrode position, Activation time). These values are then recorded and manually exported as an Excel spreadsheet. Next, the Excel spreadsheet is imported into a MATLAB program that displays activation time contour plots. Because tissue activation was not achieved in porcine experiments previous data from the Villa experiments were used to verify activation time determination method. The activation times are plotted as a function of space (mm) of the 9x9 electrode recording region. Fig. 6 shows a contour map for activation times for two sets of former porcine data. The activation contour maps show the distribution of activation times at regions of the cardiac tissue. We expected and observed increased activation times as the electrical wavefront propagated from the line of stimulation electrodes at the bottom of the display.

Conduction velocity vectors, as previously mentioned, are computed using the developed MATLAB program employing the method described by Bayly et al. [36]. Qualitative inspection of the velocity vector field shows an overall direction of flow from the line of stimulating electrodes. Fig. 6B shows the velocity vector field.

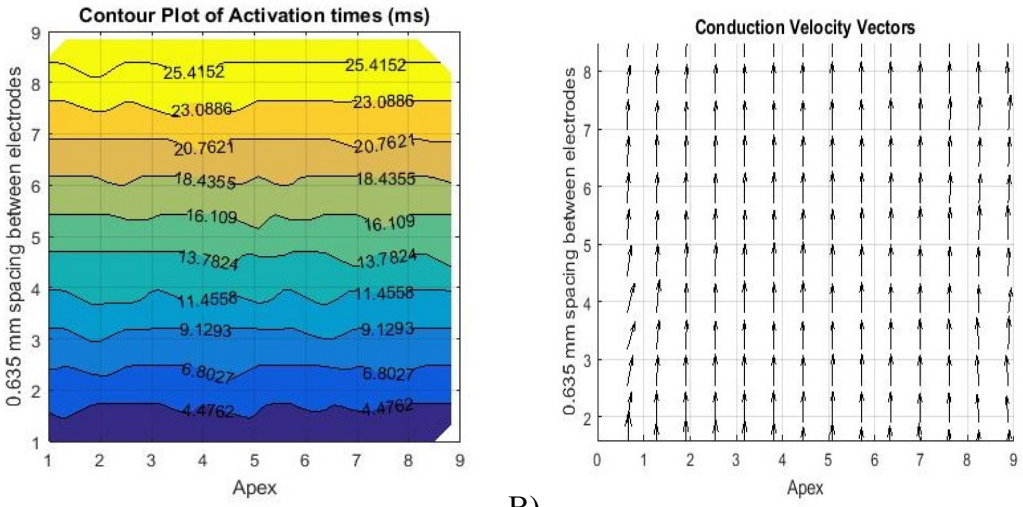

A) B)

Fig 6. (A) Contour plot of activation times (ms) of the 9x9 mapping portion of the electrode array. Stimulation occurred from the bottom of the electrode array. As expected the activation times increase as the wavefront propagates away from the line of stimulation electrodes at the bottom edge of the array. The contour plot is shown as an 8x8 square due to the polynomial fitting window used to interpolate activation times between electrodes. B) Velocity vector field plot of (A) activation time data. The electrical propagation is moving away from the stimulation row of electrodes.

C. Arrhythmic Prone Site Detection

As seen in Fig. 7 (A and B) there are no regions within the 9x9 mapping electrodes for the two porcine samples that display CV speeds that are considered abnormal. To verify the identification method of abnormal CV sites, activation times for a particular region within the 9x9 window were manually altered to slow the CV. Fig. 8 demonstrations a complete user interface display of activation time contour plot, CV vector field, CV contour plot, as well as the arrhythmic prone identification display.

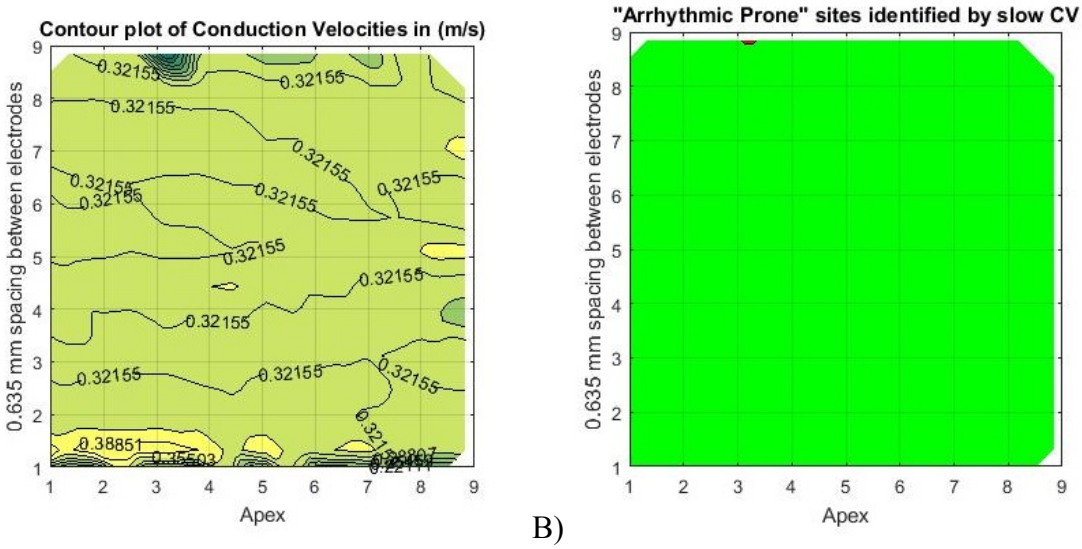

A) B)

Fig. 7. (A) Contour plot of calculated CV in m/s from Fig. 6 activation times sample data. **(B)** Arrhythmic prone site identification plot. From the calculated CV speeds in Fig. 7 A. there are no abnormally slow CV speeds detected in the data, and green, indicating normal CV, appears at all locations.

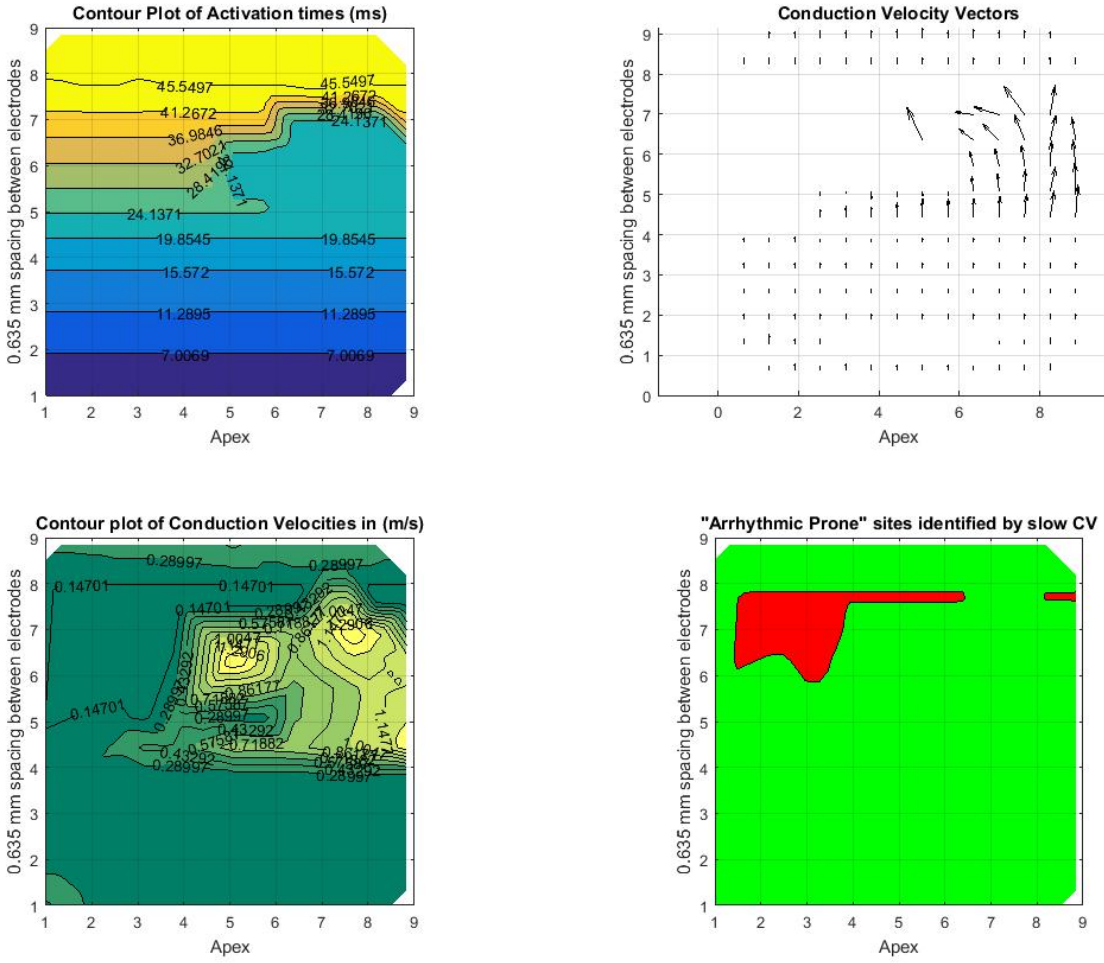

Fig. 8. Complete MATLAB interface after data is processed. This particular set of activation time data has been manipulated to slow CV speeds in the upper left hand portion of the 9x9 array. There are no vectors that appear in the upper left portion of the CV vector field due to their small magnitude. This was done in order to verify ability of the program to calculate and identify CV speeds of less than 0.08 m/s as “Arrhythmic Prone”. The red area that is identified in the “Arrhythmic Prone” site identification panel is displayed by a mechanism created in MATLAB that displays any CV speeds less than 0.08 m/s as red. Any CV calculated above 0.08 m/s is displayed in green.

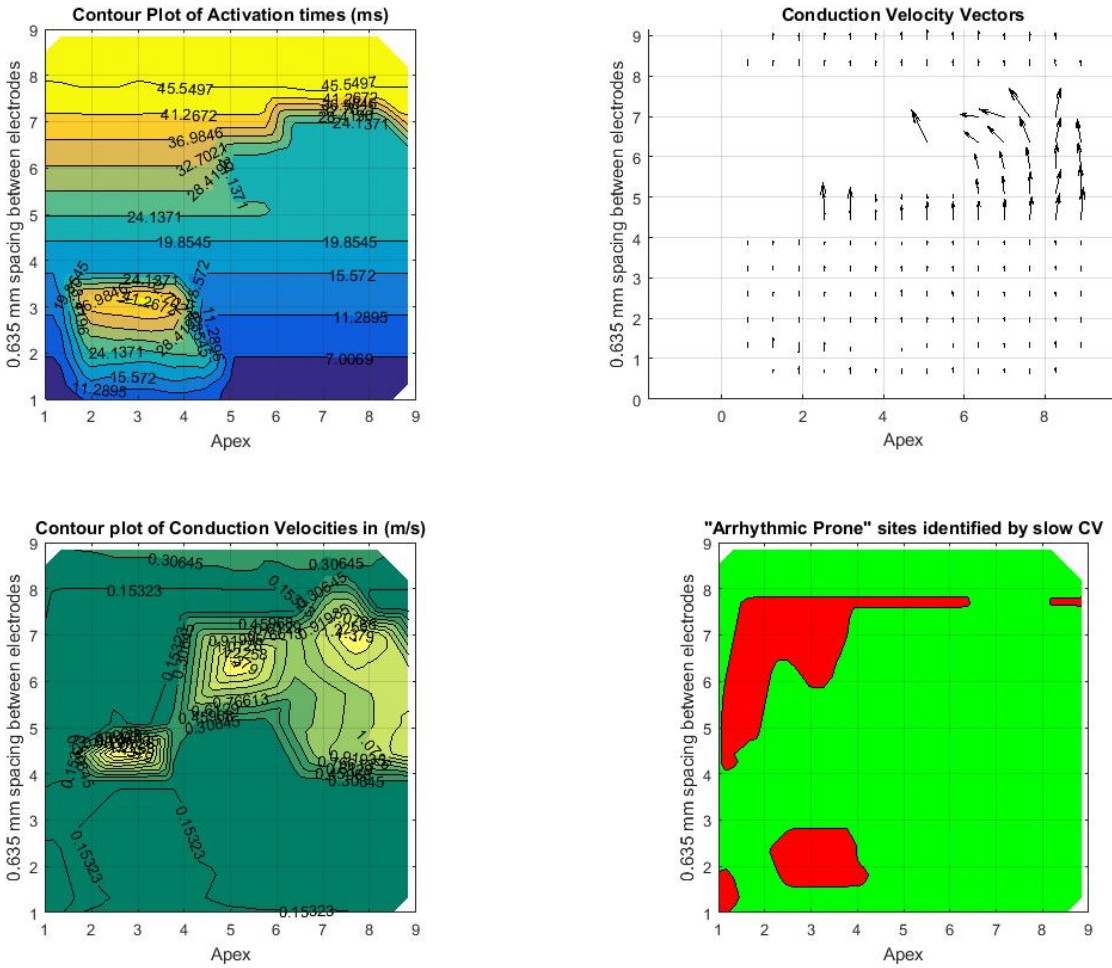

Fig. 9. Complete MATLAB interface of data that possesses two major arrhythmic prone sites based on CV speeds less than 0.08 m/s. Individual electrode activation times were manipulated in this data set to contain two areas that display abnormal CVs. There is consistency between all four panels that allow for clear interpretation of the “arrhythmic prone” sites.

IV. Discussion

We have been able to design an inexpensive electrode array that has the ability to study the electrophysiological characteristics of isolated heart tissue. Due to recent efforts in the development of engineered heart tissue patches as a potential treatment for myocardial infarction repair, there is a need for a reliable way of determining the electrical properties of isolated patches of cardiac tissue.

We have been able to develop an electrode array complete with a data acquisition and analysis program that is able to detect changes in electrical potential for individual electrodes. Mechanisms within the analysis program have the abilities to send a desired current input through selected electrodes, record the electric potential changes in the cardiac tissue sample, and assign the appropriate activation time to the individual mapping electrodes. These activation times are then translated into conduction velocities over the mapping portion of the electrode array. Finally, the program is able to identify areas within the mapping window that displays CVs that would allow a reentrant circuit to develop.

The system was verified using porcine tissue samples that were placed in a controlled tissue bath system that maintained normal physiological conditions. The system has the ability to control temperature, pH, and the circulation of the medium using a feedback control system.

The protocol for determining activation threshold is common among literature in cardiac mapping. Tissue is stimulated with an electrical current and is continually increased until an active response is achieved in the tissue sample (29, 31, 41). We followed the correct procedure for finding activation threshold but were unable to achieve tissue activation in the porcine samples. We believe this is due to the limited porcine tissue trials. We were able to verify that

that current stimulation portion of the LabVIEW allows the user the ability to change current amplitude, pulse width, and frequency.

Conduction velocity is calculated using the same method performed by Bayly *et al.* [36] and described in Methods section (II.D). This provides real-time visual feedback on the magnitude and speed of electrical propagation, and is used to indicate potential arrhythmic prone regions. There are other methods that only measure the magnitude of CV across the tissue. The visualization of the vector field enhances the ability of our system to also show the direction of electrical propagation. Future work would allow the direction of vector fields to also play a part in the identification of an arrhythmic prone site.

V. Recommendations, Limitations, Future work

One of our objectives was to expand and update previous efforts within the lab for electrical characterization of isolated cardiac tissue. We believe we have not only fulfilled this objective but have opened up more avenues for future research, in our lab, to explore.

A. Recommendations

The ability to maintain tissue sample stability within the tissue bath was not as effective over a large range of tissue sample sizes. The porcine samples that we received varied greatly in size due to variation in animal ages. This made securing the larger isolated samples difficult using the current clamps in the tissue bath. We therefore recommend searching for an alternative clamping mechanism that that easily adjusts for varying sizes of samples due to the wide age range of samples we receive in the lab.

A bath tissue system upgrade is recommended, as the viability of the cardiac tissue is essential in achieving accurate recordings. The tissue bath offers a great deal of control as far as maintaining relevant physiological conditions is concerned. This is accomplished by having multiple tubes, electrodes, meters, and wires being placed into the tissue bath. This causes an issue when trying to maneuver the electrode array to various regions of the tissue where multiple controlling components need to be held into the DMEMs solution. We suggest updating the acrylic chamber with permanent clamps to secure the various controller components in the tissue bath to enable more room for the experimenter to operate.

Currently, the “arrhythmic prone” identification mechanism is only taking CV magnitude into consideration for identifying areas that display abnormal CV. Based on literature a CV speed less that 0.08 m/s is considered abnormal. This is not the only property that can cause a reentrant

circuit. A mechanism that also characterizes the angle differences in sequential CV vectors may be useful in determining areas that may still display arrhythmic prone traits but display normal CV speeds.

B. Limitations

As previously mentioned, the number of porcine samples available to study limited our ability to be successful in observing tissue activation in our porcine sample studies. Because of this limitation we were unable to verify the cardiac tissue mapping electrode array to determine pro-arrhythmic tissue substrates using a single porcine sample. Nonetheless, we verified the electrode array by importing previously recorded data and simulating different conduction scenarios. Further studies in porcine or small animals tissues such as rat or guinea pig should be performed.

The number of mapping electrodes is limited by the number of available slots in the individual modules that are compatible with MATLAB. The 9x9-mapping surface is smaller than previous work done in the lab that used an 11x11-mapping surface. There are 144 available slots for electrodes in the current DAQ system. If the mapping surface is needed to be larger than 12x12 alternative methods must be used.

Finally, another significant limitation was the rigidity of the electrode array itself. We are trying to map using a flat surfaced electrode array on a curved surface of cardiac tissue. Slight pressure is necessary to maintain sufficient contact for all electrodes in the array. The design of a flexible electrode array may be able to alleviate this issue.

C. Future Work

This study has provided a significant upgrade within the lab for the mapping system for electrical properties in isolated cardiac tissue. The device that has been developed is intended for further cardiac mapping efforts within the lab as well as in the development and research of engineered cardiac tissue patches. These patches have been characterized mechanically [43]; the next progression before in-vivo animal models is to characterize the patches electrically.

The recent upgrades to the mapping system as well as previous efforts in the lab that have provided adequate baseline electrophysiological activity for both porcine and rats that will allow for a wide range of future cardiac mapping research.

VI. Conclusions

Advances in our understanding in both biomaterials and cellular scaffolds have opened up many novel approaches in resolving medical diseases we have today. Ex vivo characterization of these prospective approaches serve as a valuable platform for predicting the scaffold potential viability as a solution to manage myocardial infarction.

The system we have developed offers a portable and accessible option for ex-vivo electrical characterization of isolated cardiac tissue. The primary limitation in ex-vivo characterization of cardiac tissue is the time to analyze a particular recording; the programming allows for real time analysis instead of extensive offline efforts. This system has the ability to analyze the activation times of 81 mapping electrodes, calculate CV vector fields, display CV contour plots, and identify areas within the mapping window that display CV speeds that are considered “arrhythmic prone”. This system coupled with a formerly developed tissue bath system [29] allows for characterization of cardiac tissue from both rats and piglets in physiologically relevant conditions.

Results from this study will provide a foundation for future research in which arrhythmic prone sites are characterized and identified on isolated cardiac tissue/ engineered cardiac patches. The ex-vivo recognition of arrhythmic prone sites will serve as a valuable tool when determining if implanting engineered heart tissue patches are a rational solution to myocardial infarction.

REFERENCES

[1] M. Page, *BMA Illustrated Medical Dictionary*. Dorling Kindersley Plc P/B, 2002.

[2] "Heartorg Home Page." *American Heart Association*. N.p., n.d. Web. 22 Feb. 2016. <http://americanheart.org/presenter.jhtml?identifier=4478>.

[3] "About Heart Attacks." *About Heart Attacks*. N.p., n.d. Web. 14 Dec. 2015. <http://www.heart.org/HEARTORG/Conditions/HeartAttack/AboutHeartAttacks/About-Heart-Attacks_UCM_002038_Article.jsp - .VquZ2_krJD9>.

[4] CDC, NCHS. Underlying Cause of Death 1999-2013 on CDC WONDER Online Database, released 2015. Data are from the Multiple Cause of Death Files, 1999-2013, as compiled from data provided by the 57 vital statistics jurisdictions through the Vital Statistics Cooperative Program. Accessed Feb. 1, 2016.

[5] CDC. Deaths, percent of total deaths, and death rates for the 15 leading causes of death in 10-year age groups, by race and sex: United States, 2013

[6] "Heart Attack." *Symptoms: Know What's a Medical Emergency*. N.p., n.d. Web. 27 Feb. 2016. <http://www.mayoclinic.org/diseases-conditions/heart-attack/in-depth/heart-attack-symptoms/art-20047744>.

[7] CDC. State Specific Mortality from Sudden Cardiac Death: United States, 1999. MMWR. 2002; 51(6):123–126.

[8] Understand Your Risk of Heart Attack." *Understand Your Risk of Heart Attack*. American Heart Association, n.d. Web. 4 Feb. 2016.

[9] “Cardiac Medications." *Cardiac Medications*. American Heart Association, n.d. Web. 18 Feb. 2016. <http://www.heart.org/HEARTORG/Conditions/HeartAttack/PreventionTreatmentofHeartAttack/Cardiac-Medications_UCM_303937_Article.jsp#.V0iQ91fAFSV >.

[10] “Beta-Blockers”. *Beta-Blockers - Texas Heart Institute Heart Information Center*. Texas Heart Institute, n.d. Web. 8 Feb. 2016. <http://www.texasheart.org/HIC/Topics/Meds/betameds.cfm>.

[11] "Coronary Angioplasty and Stents." *Mayo Clinic*. Mayo Clinic, n.d. Web. 8 Feb. 2016. <http://www.mayoclinic.org/tests-procedures/angioplasty/basics/definition/prc-20014401>.

[12] "Coronary Artery Bypass Surgery: MedlinePlus." *U.S National Library of Medicine*. U.S. National Library of Medicine, n.d. Web. 08 Feb. 2016. <https://www.nlm.nih.gov/medlineplus/coronaryarterybypasssurgery.html>.

[13] "Coronary Artery Bypass Surgery." *Texas Heart Institute Heart Information Center*. Texas Heart Institute, n.d. Web. 09 Feb. 2016. <http://www.texasheart.org/HIC/Topics/Proced/cab.cfm>.

[14] Tracy CM, Epstein AE, Darbar D, et al. 2012 ACCF/AHA/HRS Focused Update Incorporated Into the ACCF/AHA/HRS 2008 Guidelines for Device-Based Therapy of Cardiac Rhythm Abnormalities: A Report of the American College of Cardiology Foundation/American Heart Association Task Force on Practice Guidelines and the Heart Rhythm Society. *J Am Coll Cardiol.* 2013; 61(3):e6-e75. doi: 10.1016/j.jacc.2012.11.007.

[15] "Implantable Cardioverter Defibrillators and Cardiac Resynchronisation Therapy for Arrhythmias and Heart Failure." *Implantable Cardioverter Defibrillators and Cardiac Resynchronisation Therapy for Arrhythmias and Heart Failure*. National Institute of Health and Care Excellence, June 2014. Web. 08 Feb. 2016. <http://www.nice.org.uk/guidance/ta314>.

[16] "Arrhythmia." Arrhythmia-PubMed Health. U.S. National Library of Medicine, n.d. Web. 30 June 2015. <http://www.ncbi.nlm.nih.gov/pubmedhealth/PMH0062940/>

[17] R. Mandapati, A. Skanes, J. Chen, O. Berenfeld. J. Jalife "Stable microreentrant sources as a mechanism of atrial fibrillation in the isolated sheep heart", Circulation, vol. 101, pp.194 -199 2000

[18] R. A. Gray, A. M. Pertsov. J. Jalife "Spatial and temporal organization during cardiac fibrillation", Nature, vol. 392, pp.75 -78 1998

[19] A. C. Skanes, R. Mandapati, O. Berenfeld, J. M. Davidenko J. Jalife "Spatiotemporal periodicity during atrial fibrillation in the isolated sheep heart", Circulation, vol. 98, pp.1236 -1248 1998

[20] Schotten, U., S. Verheule, P. Kirchhof. A. Goette. "Pathophysiological Mechanisms of Atrial Fibrillation: A Translational Appraisal." *Physiological Reviews* 91.1 (2011): 265-325. Web.

[21] Rohr, S. Role of gap junctions in the propagation of the cardiac action potentials. Cardiovasc. (2004); Res.62, 309-322. doi: 10.1016/j.cardiores.2003.11.035

[22] Greisas, A.; Zafrir, Z.; Zlochiver, S., "Detection of Abnormal Cardiac Activity Using Principal Component Analysis–-A Theoretical Study," Biomedical Engineering, IEEE Transactions on, vol.62, no.1, pp.154, 164, Jan. 2015 doi: 10.1109/TBME.2014.2342792

[23] Kleber, A. G. "Basic Mechanisms of Cardiac Impulse Propagation and Associated Arrhythmias." *Physiological Reviews* 84.2 (2004): 431-88. Web. 2 Mar. 2015.

[24] Mendis, S., K. Thygesen, K. Kuulasmaa, S. Giampaoli, M. Mahonen, K. Ngu Blackett. L. Lisheng. "World Health Organization Definition of Myocardial Infarction: 2008-09 Revision." *International Journal of Epidemiology* 40.1 (2010): 139-46. Web. 2 Mar. 2016.

[25] Patel, Nikita M., Iman K. Yazdi, Ennio Tasciotti. Ravi K. Birla. "Optimizing Cell Seeding and Retention in a Three-dimensional Bioengineered Cardiac Ventricle: The Two-stage Cellularization Model." *Biotechnol. Bioeng. Biotechnology and Bioengineering* (2016): n. pag. Web. 5 May 2016.

[26] Marc N. Hirt, Arne Hansen, Thomas Eschenhagen. "Cardiac Tissue Engineering: State of the Art". Circulation Research. 2014;114:354-367, doi:10.1161/CIRCRESAHA.114.300522

[27] "Arrhythmia." Arrhythmia-PubMed Health. U.S. National Library of Medicine, n.d. Web. 30 June 2015. <http://www.ncbi.nlm.nih.gov/pubmedhealth/PMH0062940/>.

[28] Attin, Mina, and William T. Clusin. "Basic Concepts of Optical Mapping Techniques in Cardiac Electrophysiology." *Biological research for nursing* 11.2 (2009): 195–207. *PMC*. Web. 08 Feb. 2016.

[29] Villa, Emanuel M.S. The University of Memphis. August 2011 Master of Science. Design of a tissue bath system for electrophysiologic characterization of isolated cardiac tissue. Major Professor: Amy L. de Jongh Curry, Ph.D.

[30] "Editorial Board." *Circulation: Arrhythmia and Electrophysiology* 4.4 (2011): 421. *American Heart Association*. Web. 08 Feb. 2016.

[31] N. Bursac et al., "Cardiac muscle tissue engineering: toward an in vitro model for electrophysiological studies," *The American Journal of Physiology*, vol. 277, no. 2 Pt 2, pp. H433-444, Aug. 1999.

[32] R. A. Malkin, "Constructing a multichannel electrocardiography system from a few standardized, high-level components," *IEEE Engineering in Medicine and Biology Magazine: The Quarterly Magazine of the Engineering in Medicine & Biology Society*, vol. 17, no. 1, pp. 34-38, Feb. 1998.

[33] S. M. Blanchard, W. M. Smith, R. J. Damiano, D. W. Molter, R. E. Ideker. J. E. Lowe, "Four digital algorithms for activation detection from unipolar epicardial electrograms," *IEEE Transactions on Bio-Medical Engineering*, vol. 36, no. 2, pp. 256- 261, Feb. 1989.(34) M. Shenasa, M. Borggrefe, G. Breithardt, *Cardiac Mapping*, Illustrated 36 edition. Wiley-Blackwell, 1994.

[35] Barnette, A.R.;Bayly, P.V.;Zhang, S.;Walcott, G.P.;Ideker, R.E.;Smith, W.M.Estimation of 3D conduction velocity vector fields from cardiac mapping data, Computers in Cardiology, 1998, 605-608. (Pubitemid 128651440)

[36] P. V. Bayly, B. H. KenKnight, J. M. Rogers, R. E. Hillsley, R. E. Ideker, W. M. Smith, "Estimation of conduction velocity vector fields from epicardial mapping data," *IEEE Transactions on Bio-Medical Engineering*, vol. 45, no. 5, pp. 563-571, May. 1998.

[37] D. Li, S. Fareh, T. K. Leung, S. Nattel, “Promotion of atrial fibrillation by heart failure in dogs: atrial remodeling of a different sort,” *Circulation*, vol. 100, no. 1, pp. 87-95, Jul. 1999.

[38] Lammers WJEP, Schalij MJ, Kirchhof CJHJ, Allessie MA. Quantifi- cation of spatial inhomogeneity in conduction and initiation of reentrant atrial arrhythmias. *Am J Physiol*. 1990; 259(*Heart Circ Physiol* 28): H1254 –H1263.

[39] A. Shiroshita-Takeshita, M. Sakabe, K. Haugan, J. K. Hennan, S. Nattel, “Model-Dependent Effects of the Gap Junction Conduction-Enhancing Antiarrhythmic Peptide Rotigaptide (ZP123) on Experimental Atrial Fibrillation in Dogs,” *Circulation*, vol. 115, no. 3, pp. 310-318, Jan. 2007.

[40] Rensma, P. L., M. A. Allessie, W. J. Lammers, F. I. Bonke, M. J. Schalij. "Length of Excitation Wave and Susceptibility to Reentrant Atrial Arrhythmias in Normal Conscious Dogs." *Circulation Research* 62.2 (1988): 395-410. Web.

[41] Leslie Hunt Fitch, “Hyperaldosteronism-Induced Cardiac Remodeling: Role in Arrhythmogenesis,” Dissertation for the Doctor of Philosophy Degree, University of Memphis, 2010.

[42] R. A. Rhoades D. R. Bell, *Medical Physiology: Principles for Clinical Medicine*, Third. Lippincott Williams & Wilkins, 2008.

[43] Wang, Bo et al. “Myocardial Scaffold-Based Cardiac Tissue Engineering: Application of Coordinated Mechanical and Electrical Stimulations.” *Langmuir : the ACS journal of surfaces and colloids* 29.35 (2013): 10.1021/la401702w. *PMC*. Web. 2 May 2016.

APPENDICES

A. List of abbreviations

CHD: coronary heart disease

ICD: Implantable cardioverter-defibrillator

EHT: Engineered heart tissue

CV: conduction velocity

ECG: electrocardiogram

MI: myocardial infarction

DMEM: Dulbecco's Modified Eagle's Medium

VI: Virtual instrument

B. Protocol for isolated porcine heart tissue mapping.

Date: _____ Weight (grams): _____ Piglet number: _____

Time of death: _____

1) Prepare medium and saline in warm bath (room 316) and wait for them to reach 37°C.□
2) Prepare bath close to mapping system with warm water, and connect necessary cables.
3) Pick up heart from Dr. Buddington, psychology building. Place in ice and transport to Engineering Technology Building.□
4) Prepare bath with warmed DMEM, place temperature controller and turn on Hot plate and pH Controller.□
5) Rinse in warmed saline. Section LV tissue. Place in bath.□Time: _____, pH:_____, Temperature: _____□
6) After 5-10 min. Rare spontaneous beating, determine threshold value. Run 5 seconds pacing at 1 beat per second, Recording last 4s, start at 0.5 mA amplitude and increase by 0.1mA until active response achieved.□
Time:_____,Threshold value: _____
7) Run two 5 seconds pacing episodes
□Filenames: _____ _____ □
pH:_____, Temperature_____ □
8) Run two 10 seconds pacing episodes
Filenames: _____ _____
□pH:_____, Temperature_____ □
9) Run two 20 seconds pacing episodes
Filenames: _____ _____
□pH:_____, Temperature_____ □
10) Run two 60 seconds pacing episodes
□Filenames: _____ _____ □
pH:_____, Temperature_____ □
11) Run two 300 seconds pacing episodes
□Filenames: _____ _____
pH:_____, Temperature_____ □

C. MATLAB program developed to obtain conduction velocity.

```
%Matlab code to obtain the conduction velocity vector fields and mean
%conduction velocities%
%Thomas Shannon Fall 2015-Spring 2016
clear all

%insert excel file with raw data%
data=xlsread('data.xls');

%maxt=maximum time%
%mint=minumum time%
maxt=max(data(:,3));
mint=min(data(:,3));

%countour data
contourx=data(:,1);
contoury=data(:,2);
contourz=data(:,3);

%The following Polynomial fitting work completed by Emanuel Villa and
%edited by Thomas Shannon
% create variable to calculate the length of the data LOD=length(data)%
LOD=length(data);
for i=1:LOD,
      V=data(i,:);
   count=0;clear window; clear window2;
   for j=1:LOD,
      if(abs(data(j,1)-V(1))<3 && abs (data(j,2)-V (2))<3 && abs(data(j,3)-V (3))<4)
         count=count+1;
         window(count,:)=data(j,:);
      end
   end
   if length(window)>8
      variance(i,1)=var(window(:,3));
      av_keep=(window(:,3)>0);
      Sums=sum(window(:,3).*av_keep);
      countav=sum(av_keep);
      average(i,1)=Sums./countav;
      count2=0;
      for k=1:length(window(:,1))
         if window(k,3)>(0.3*average(i)) && window (k,3)<(1.7*average(i))
            count2=count2+1;
            window2(count2,:)=window(k,:);
            %remake the array from window data%
```

```
            if exist('CT','var')
                CT=[CT;window2(count2,:)];
            else
                CT(1,:)=window2(1,:);
            end
        end
    end
    modelterms=[2 0;0 2;1 1;1 0;0 1;0 0];
    polymodel2=polyfitn(window2(:,1:2),window2(:,3),modelterms);
    %polyfitn function downloaded from internet%
    a=polymodel2.Coefficients(1);
    b=polymodel2.Coefficients(2);
    c=polymodel2.Coefficients(3);
    d=polymodel2.Coefficients(4);
    e=polymodel2.Coefficients(5);
    f=polymodel2.Coefficients(6);
    x=data(i,1);
    y=data(i,2);
    Tx=2*a*x+c*y+d;
    Ty=2*b*y+c*x+e;
    Vx(i,1)=Tx/(Tx*Tx+Ty*Ty);
    Vy(i,1)=Ty/(Tx*Tx+Ty*Ty);
    vel(i,:)=[x,y,Vx(i),Vy(i)];
    mag(i,1)=sqrt(((Vx(i))^2)+((Vy(i))^2));
    R2(i,1)=polymodel2.R2;
    RMSE(i,1)=polymodel2.RMSE;
    NRMSE(i,1)=polymodel2.RMSE/(maxt-mint);
    Z(i,1)=a*data(i,1).^2+b*data(i,2).^2+c*data(i,1).*data(i,2)+d*data(i,1)+e.*data(i,2)+f;
    resid(i,1)=abs(Z(i,1)-data(i,3));
    if (R2(i)<0||abs(mag(i))>3||resid(i)>1||isnan(resid(i)))
        velcorr(i,:)=[0,0,0,0];
        mag(i,1)=0;
        resid(i,1)=0;
        R2(i,1)=0;
    else
        velcorr(i,:)=vel(i,:);
        mag(i,1)=sqrt(((Vx(i))^2)+((Vy(i))^2));
        resid(i,1)=abs(Z(i,1)-data(i,3));
        R2(i,1)=polymodel2.R2;
    end
  end
  count=0;
end

X=velcorr(:,1); Y=velcorr(:,2); VX=velcorr(:,3); VY=velcorr(:,4);
```

```
%Thomas Shannon
%Activation Time contour
AT=subplot(2,2,1)
xv = linspace(1, 9, 50);
yv = linspace(1, 9, 50);
[Xinterp,Yinterp] = meshgrid(xv,yv);
Zinterp = griddata(contourx,contoury,contourz,Xinterp,Yinterp);
contourf(Xinterp,Yinterp,Zinterp);
[c,h]=contourf(Xinterp,Yinterp,Zinterp, 10); clabel(c,h);
% Adds contour level labels on

grid on
colormap(AT,parula(10))
axis equal
title('Contour Plot of Activation times (ms)')
xlabel('X axis (0.635 mm spacing between electrodes)')
ylabel('Y axis')

%AT contour w/ CV vectors
CVV=subplot (2,2,2)
hold on
quiver(X,Y,VX,VY,1,'black')
hold off
grid on
axis equal
title('Conduction Velocity Vectors')
xlabel('X axis (0.635 mm spacing between electrodes)')
ylabel('Y axis')

%CV Contour
CV=subplot(2,2,3)%
VX=velcorr(:,3);
VY=velcorr(:,4);
AVX=abs(VX);
AVY=abs(VY);
AP=sqrt(AVX.^(2)+AVY.^(2));              %ABSOLUTE VELOCITY OF VECTORS

xx = linspace(1, 9, 50);
yy = linspace(1, 9, 50);
[Xinterp,Yinterp] = meshgrid(xx,yy);
AZinterp = griddata(X,Y,AP,Xinterp,Yinterp);
contourf(Xinterp,Yinterp,AZinterp);
[C,h]=contourf(Xinterp,Yinterp,AZinterp, 10); % Adds contour level labels on
v=[0.08];
clabel(C,h,'Font size',14,'Color','Red');
```

```
            % CV identified at 0.08 M/sec as Arryhthmic prone.
              %Forces a contour if any CV values are found at 0.08 M/sec
               % CV identified at 0.08 M/sec as Arryhthmic prone.
grid on
colormap(CV,summer(6))
axis equal
axis tight
xlabel('X axis (0.635 mm spacing between electrodes)')
ylabel('Y axis')
title('Contour plot of Conduction Velocities in (m/s)')


%"AP" indentifier
API=subplot(2,2,4)%
contourf(Xinterp,Yinterp,AZinterp, [min(AZinterp(:)); .08]);
colormap([1,0,0; 0,1,0])



grid on
axis equal
axis tight
xlabel('X axis (0.635 mm spacing between electrodes)')
ylabel('Y axis')
title('"Arrhythmic Prone" sites identified by slow CV')
```

D. Preliminary data using saline solution.

Prior to porcine experiments, bench tests were performed in saline solution to verify current stimulation waveform through the peripheral row of electrodes as well as confirm individual electrode recordings. For this experiment, the electrode array was suspended freely in a beaker of saline solution. The following results verify we were able to deliver current through the stimulation row of electrodes as well as record the voltage potential in the 81 mapping electrodes seen in Fig. 10. In Fig. 11 we have our initial, or bench test, peak detector configured to determine the stimulus artifact in saline solution. In porcine experiments, we changed the peak detector criteria to determine tissue activation rather than stimulus artifact.

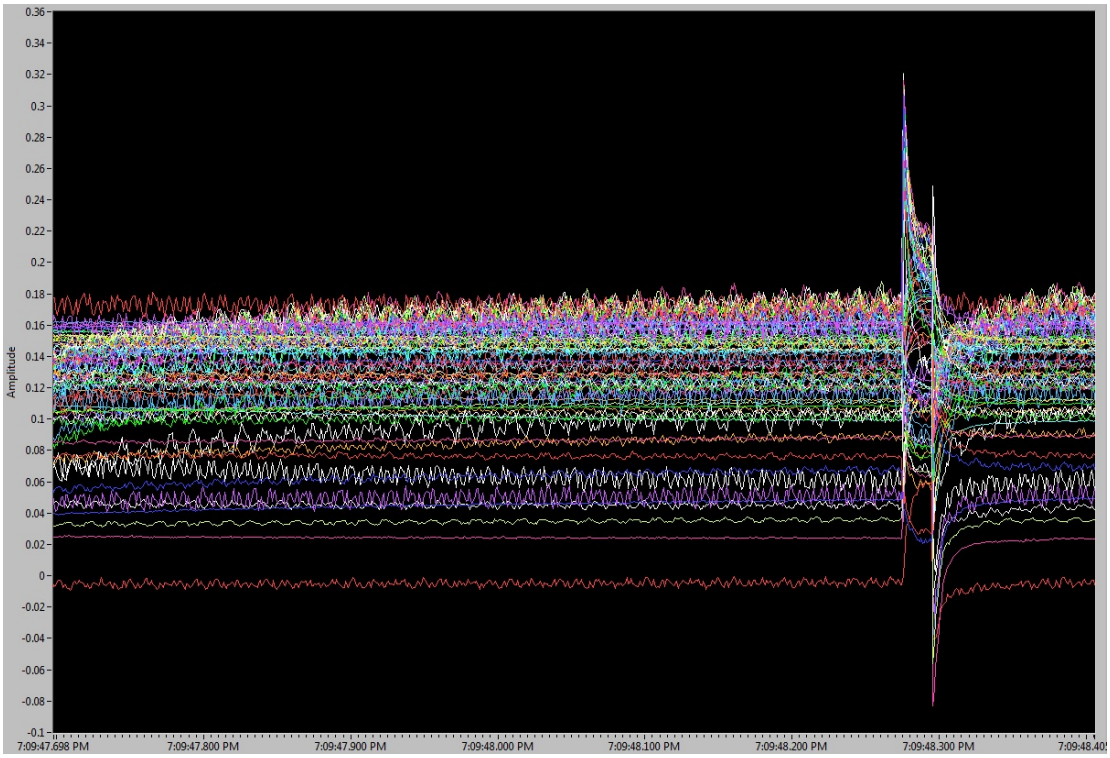

Fig. 10. Preliminary LABVIEW display showing voltage response to a single square wave current pulse in saline solution for 81 mapping electrodes. The large deflection seen is the stimulus artifact from the current pulse.

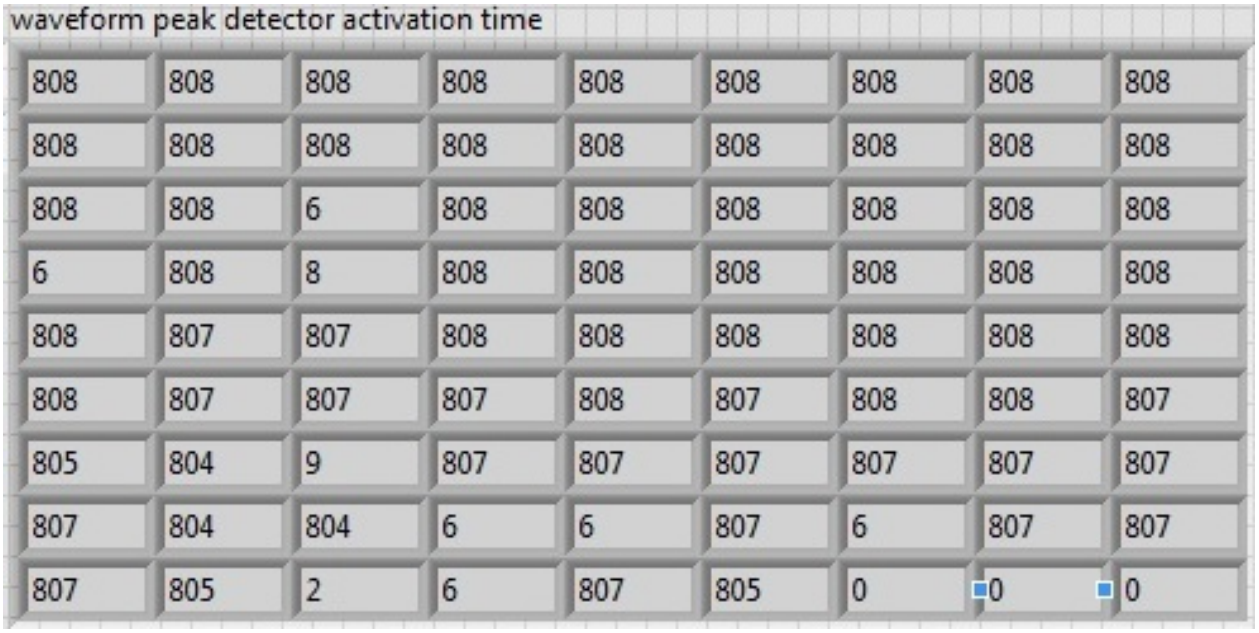

Fig. 11. Peak times of 81 mapping electrode recordings in saline solution experiments. The table represents the spatial location of the 9x9 array of electrodes. The peak detector was configured to detect stimulus artifact and 70 out of the 81 recordings show peak time of 804-808 ms. This is consistent with the time of the leading edge of the stimulus waveform in 70 recordings